Communicating with Intelligent Surfaces

Communicating with Intelligent Surfaces

Davide Dardari
DEI, CNIT, University of Bologna, I-47521 Cesena, Italy. Email: davide.dardari@unibo.it

***Abstract*—This paper analyzes the fundamental communication problem involving large intelligent surfaces (LIS) starting from electromagnetic (e.m.) arguments. Since the numerical solution of the corresponding optimal eigenfunction problem is in general computationally prohibitive, simple but accurate analytical expressions for the link gain and available degrees-of-freedom (DoF) are derived. It is shown that the achievable DoF and gain offered by the wireless link are determined only by geometric factors, and that the classic Friis' formula is no longer valid in this scenario where the transmitter and receiver could operate in the near-field regime. Furthermore, results indicate that, contrarily to classic MIMO systems, when using LIS more than one DoF might be available in strong line-of-sight (LOS) channel conditions, which corresponds to a significant increase of spatial capacity density.**

I. Introduction

Future wireless networks are expected to become distributed intelligent communication, sensing and computing entities. This will allow to meet ultra-reliability, high capacity densities, extremely low-latency and low-energy consumption requirements posed by emerging application scenarios such as that of Industrial Internet of Things in Factories of the Future [1]. The current trend to satisfy part of such requirements is through cell densification, massive multiple-input multiple-output (MIMO) transmission, and the exploitation of higher frequency bands (e.g., millimeter and THz) [2]. Unfortunately, when moving to higher frequency bands the channel path-loss increases and the multipath becomes sparse so that the spatial multiplexing peculiarity of MIMO, i.e., the channel degrees-of-fredom (DoF), guaranteed at lower frequencies by rich multipath, is lost in favor of only beamforming gain, which increases the communication capacity logarithmically instead of linearly with the number of antennas [3].

Recently, the introduction of reconfigurable meta-surfaces to realize, for instance, smart electromagnetic (e.m.) reflectors, large configurable antennas, using thin meta-materials has opened new very appealing perspectives [4]–[8]. In fact, with meta-materials e.m. waves can be shaped almost arbitrarily, at least in theory. These *intelligent surfaces* can be embedded in daily life objects such as walls, clothes, buildings, etc., and can be used as distributed platforms to perform low-energy and low-complexity sensing, storage and analog computing. Environments coated with intelligent surfaces constitute the recently proposed *smart radio environments* concept [9], [10]. In smart radio environments, the design paradigm is changed from wireless devices/networks that adapt themselves to the environment (e.g., propagation conditions), to the joint optimization of both devices and environment using reconfigurable intelligent surfaces.

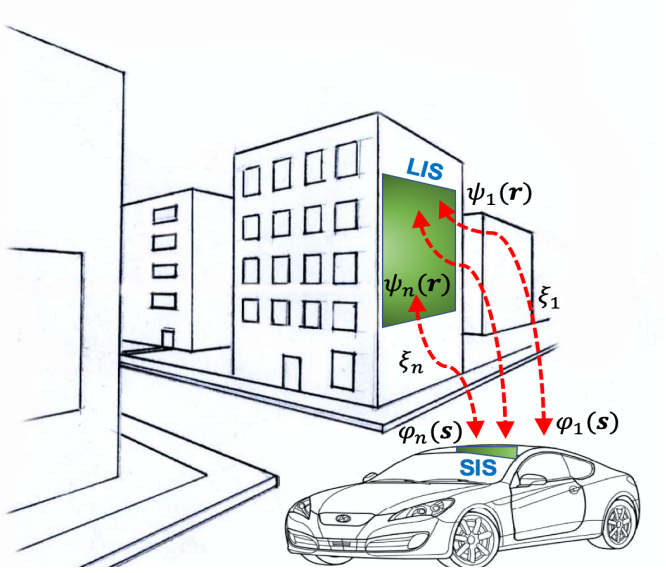

Fig. 1. Typical scenario employing LIS-based antennas.

In this context, most of papers deal with intelligent surfaces used to assist multipath propagation, i.e., as reconfigurable reflectors [9], [10]. A rich literature considering meta-surfaces to realize refrectarrays or trasmitarrays antennas is also available, where the e.m. wave, emitted by a single antenna element close to the surface, is reflected/refracted by the meta-surface in order to obtain flexible beamforming or focusing functionalities at low complexity [7], [11]. Along a different direction, in [12] a general theory of space-time modulated digital coding meta-surfaces to achieve simultaneous manipulations of e.m. waves in both space and frequency domains is proposed and validated in the far-field regime. Less papers analyze the potential of using meta-surfaces as large intelligent surface (LIS) antennas [13]. LISs (e.g., on walls), medium intelligent surfaces (MISs) (e.g., on cars/truck), and small intelligent surfaces (SISs) (e.g., on smartphones/sensors), provide a great opportunity to move towards the ultimate capacity limit of the wireless channel.

When considering a LIS, classic models for antenna arrays fail to capture the actual wireless link characteristics in terms of gain, path-loss and available DoF as they assume (Fraunhofer) far-field condition (i.e., a distance much larger than the antenna dimension so that waves can be considered plane [14]), whereas with LISs the size of the antenna becomes comparable to the distance of the link (near-field regime). Moreover, such models usually do not account for the flexibility in generating the current distribution offered by LISs and hence common results from aperture antennas

theory are no longer valid. Therefore, new models based on the ultimate physical limitation brought by the e.m. transportation of information should be considered. The main fundamental results on e.m. transportation of information can be found in [15] and references therein. These results mainly address the computation of the spatial dimensionality of the e.m. field when considering finite volumes with sources and scatterers in the far-field, but they do not consider the DoF available in a communication system employing intelligent surfaces.

One of the earliest works proposing and studying LISs for communication is [13], which considers the communication between a single-antenna user with a LIS and where an analysis of the spatial capacity density is presented. Practical aspects related to the design of the optimal sampling lattice of the LIS are considered by showing that the hexagonal lattice is optimal for minimizing the surface-area of a LIS under the constraint that one independent signal dimension should be obtained per spent antenna element of the LIS.

The issue of power and cost of large massive MIMO systems using meta-surfaces is addressed in [8]. Such challenges are tackled by incorporating signal processing methods, such as compression and analog combining, in the physical antenna structure. The characterization of the maximal achievable sum-rate on the uplink and potential gain over standard antenna arrays are studied.

At author knowledge, no results are present related to the investigation of the available DoF as well as the coupling gain between intelligent surfaces, in particular when one of them is large and hence it might operate in the near-field.

In this paper, the optimal communication between LIS/SIS is addressed as an eigenfunction problem starting from an e.m. formulation. Unfortunately, finding the solution to the eigenfunction problem requires extensive and sometimes prohibitive e.m.-level simulations when large surfaces are considered, and usually they do not provide general insights. Therefore, we focus on obtaining approximate analytical but accurate expressions for the link gain and the available orthogonal communication modes (i.e., DoF) between the transmitter and receiver. Although such expressions are easy to compute numerically, we further derive close-form expressions for some specific cases of interest which allow to get important insights about the communication between intelligent surfaces and can serve as design guidelines in future wireless networks employing LISs.

In the rest of the paper we use the following notation: Lowercase bold variables denote vectors in the 3D space, i.e., $\mathbf{r} = \mathbf{u}_x \cdot r_x + \mathbf{u}_y \cdot r_y + \mathbf{u}_z \cdot r_z$ is a vector with cartesian coordinates (r_x, r_y, r_z), $\hat{\mathbf{r}}$ is a unit vector denoting its direction, and $r = |\mathbf{r}|$ denotes its magnitude, where $\hat{\mathbf{u}}_x$, $\hat{\mathbf{u}}_y$ and $\hat{\mathbf{u}}_z$ represent the unit vectors in the x, y and z directions, respectively. Italic capital letters (e.g., $E(\mathbf{r})$, $J(\mathbf{r})$) represent electromagnetic vector functions. Boldface capital letters are matrices (e.g., $\mathbf{H}$), where $\mathbf{I}$ is the identity matrix, and † indicates the conjugate transpose operator. $\nabla^2 J(\mathbf{r})$ is the Laplacian of the vector function $J(\mathbf{r})$. Surfaces and volumes are indicated with calligraphic letters $\mathcal{S}_\mathrm{T}$, where $A_\mathrm{T} = |\mathcal{S}_\mathrm{T}|$ is their Lebesgue measure. Define the $\mathcal{L}_2$-norm $||\mathbf{r}||$, the Frobenius norm $||\mathbf{X}|| = \sqrt{\sum_{k=1}^{N}\sum_{j=1}^{N}\left|\{\mathbf{X}\}_{kj}\right|^2}$, and the outer product (tensor product) $\mathbf{r}\otimes\mathbf{s}$, where $\{\mathbf{r}\otimes\mathbf{s}\}_{kj} = r_k\, s_j$, and $\{\mathbf{X}\}_{kj}$ is the kjth element of matrix $\mathbf{X}$. Moreover, denote with μ, ϵ, and $\eta = \sqrt{\mu/\epsilon}$ the permittivity, permeability and impedance of free-space, respectively, and c the speed-of-light.

II. General Problem Formulation

Thanks to the adoption of meta-materials, with LISs one can synthesize in principle any current distribution, then it is of interest to investigate how many orthogonal channels, i.e., communication modes or DoF, are possible when two LIS/SIS are communicating with each other. To this purpose, we approximate the intelligent surface as a continuous array of an infinite number of infinitesimal antennas.

A. Problem Formulation

Consider a transmit MIS/SIS antenna with surface $\mathcal{S}_\mathrm{T}$ of area $A_\mathrm{T} = |\mathcal{S}_\mathrm{T}|$ containing e.m. monochromatic source currents with Fourier representation $J(\mathbf{s},\omega)$ different from zero in $\mathbf{s}\in\mathcal{S}_\mathrm{T}$, with ω being the angular frequency, which generate an electric field $E(\mathbf{r},\omega)$ in free-space. In addition, consider a receive LIS antenna $\mathcal{S}_\mathrm{R}$ not intersecting $\mathcal{S}_\mathrm{T}$, with area $A_\mathrm{R} = |\mathcal{S}_\mathrm{R}|$. Due to the reciprocity of the radio medium, their role can be exchanged.

Each frequency component satisfies the inhomogeneous Helmholtz wave equation[1]

$$\nabla^2 E(\mathbf{r}) + k_0^2\, E(\mathbf{r}) = \jmath k_0\, \eta\, J(\mathbf{r}), \tag{1}$$

where $k_0 = \omega/c = 2\pi/\lambda$ is the wavenumber, λ the wavelength, and we have dropped the explicit dependence on ω to lighten the notation.

Any point source in $\mathcal{S}_\mathrm{T}$ generates the (outgoing) wave given by the tensor Green's function [14]

$$G(\mathbf{r}) = -\frac{\jmath\omega\mu}{4\pi}\left[\mathbf{I} + \frac{1}{k_0}\nabla\nabla\right]\frac{\exp(-\jmath k_0 r)}{r}, \tag{2}$$

with $r = |\mathbf{r}|$, which obeys the Helmholtz equation.

By expanding (2) it is [17]

$$G(\mathbf{r}) = -\frac{\jmath\,\eta\exp(-\jmath k_0 r)}{2\lambda r}\left[\left(\mathbf{I} - \hat{\mathbf{r}}\cdot\hat{\mathbf{r}}^\dagger\right) + \frac{\jmath\lambda}{2\pi r}\left(\mathbf{I} - 3\,\hat{\mathbf{r}}\cdot\hat{\mathbf{r}}^\dagger\right)\right. \tag{3}$$

$$\left. -\frac{\lambda^2}{(2\pi r)^2}\left(\mathbf{I} - 3\,\hat{\mathbf{r}}\cdot\hat{\mathbf{r}}^\dagger\right)\right] \simeq -\frac{\jmath\,\eta\exp(-\jmath k_0 r)}{2\lambda r}\left(\mathbf{I} - \hat{\mathbf{r}}\cdot\hat{\mathbf{r}}^\dagger\right),$$

where we grouped the terms multiplying, respectively, the factors $1/r$, $1/r^2$ and $1/r^3$. It is evident from (3) that when $r \gg \lambda$, the second and third terms can be neglected and hence the right-hand side approximation in (3) holds.[2] By adding all the waves from the sources in $\mathcal{S}_\mathrm{T}$, the resulting wave in $\mathbf{r}$ is

$$E(\mathbf{r}) = \int_{\mathcal{S}_\mathrm{T}} G(\mathbf{r}-\mathbf{s})\, J(\mathbf{s})\, d\mathbf{s}\,. \tag{4}$$

[1] Similar formulation can be done for the magnetic field in case of magnetic currents even though it is always possible to model the problem using equivalent source currents [16].

[2] Under this condition the system does not work in the 'reactive' near-field.

The goal is to determine how many orthogonal waves, namely DoF, can be activated between $\mathcal{S}_\mathrm{T}$ and $\mathcal{S}_\mathrm{R}$, as well as the corresponding coupling intensity. To determine the dimensionality of the waves, one has to solve the following coupled eigenfunction problem [18], [19]

$$\xi^2 J(\mathbf{s}) = \int_{\mathcal{S}_\mathrm{T}} K_\mathrm{T}(\mathbf{s},\mathbf{s}')\, J(\mathbf{s}')\, d\mathbf{s}' \tag{5}$$

$$\xi^2 E(\mathbf{r}) = \int_{\mathcal{S}_\mathrm{R}} K_\mathrm{R}(\mathbf{r},\mathbf{r}')\, E(\mathbf{r}')\, d\mathbf{r}', \tag{6}$$

where

$$K_\mathrm{T}(\mathbf{s},\mathbf{s}') = \int_{\mathcal{S}_\mathrm{R}} G^\dagger(\mathbf{r}-\mathbf{s})\, G(\mathbf{r}-\mathbf{s}')\, d\mathbf{r} \tag{7}$$

$$K_\mathrm{R}(\mathbf{r},\mathbf{r}') = \int_{\mathcal{S}_\mathrm{T}} G(\mathbf{r}-\mathbf{s})\, G^\dagger(\mathbf{r}'-\mathbf{s})\, d\mathbf{s}\,. \tag{8}$$

Since $K_\mathrm{T}(\mathbf{s},\mathbf{s}')$ and $K_\mathrm{R}(\mathbf{r},\mathbf{r}')$ are Hermitian kernels, a set of eigenfunctions $\{\phi_n(\mathbf{r})\}$, $\{\psi_n(\mathbf{s})\}$ with real eigenvalues ξ_1^2, ξ_2^2, ..., solution of (5) and (6) exists. Specifically, any current density and wave in $\mathcal{S}_\mathrm{T}$ and $\mathcal{S}_\mathrm{R}$ can be written, respectively, as

$$J(\mathbf{r}) = \sum_n a_n\, \phi_n(\mathbf{r}) \qquad E(\mathbf{r}) = \sum_n b_n\, \psi_n(\mathbf{r}), \tag{9}$$

where $\{\phi_n(\mathbf{r})\}$ and $\{\psi_n(\mathbf{r})\}$ are two sets of orthonormal (vector) functions that are complete, respectively, in $\mathcal{S}_\mathrm{T}$ and $\mathcal{S}_\mathrm{R}$, i.e.,

$$\int_{\mathcal{S}_\mathrm{T}} \phi_n(\mathbf{r})\, \phi_m^\dagger(\mathbf{r})\, d\mathbf{r} = \delta_{nm} \qquad \int_{\mathcal{S}_\mathrm{R}} \psi_n(\mathbf{r})\, \psi_m^\dagger(\mathbf{r})\, d\mathbf{r} = \delta_{nm}\,. \tag{10}$$

Each solution is a spatial dimension of the system across which one can establish an orthogonal communication (see Fig. 1). Since the surfaces $\mathcal{S}_\mathrm{T}$ and $\mathcal{S}_\mathrm{R}$ are finite, in practice the number D of DoF, i.e., the number of eigenvalues ξ_n^2 different from zero, is finite.

The geometric interpretation is that the generic source current $J(\mathbf{s})$ can be projected onto the coordinate system determined by the orthogonal (vector) eigenfunctions $\{\phi_n(\mathbf{s})\}$ then, through the tensor $G(\mathbf{r})$ in (4), the nth eigenfunction $\phi_n(\mathbf{s})$ of surface $\mathcal{S}_\mathrm{T}$ is put in one-to-one correspondence with the nth eigenfunction $\psi_n(\mathbf{r})$ of the receive surface $\mathcal{S}_\mathrm{R}$ through the scaling singular value ξ_n. Therefore, if one takes as source function the nth eigenfunction, i.e., $J(\mathbf{s}) = \phi_n(\mathbf{s})$, $\mathbf{s} \in \mathcal{S}_\mathrm{T}$, then the output electric field results $\xi_n\, \psi_n(\mathbf{r})$, $\mathbf{r} \in \mathcal{S}_\mathrm{R}$. In general it is $b_n = \xi_n\, a_n$.

The eigenfunction decomposition ensures the maximum level of coupling between the sources in $\mathcal{S}_\mathrm{T}$ and the field in $\mathcal{S}_\mathrm{R}$, so that the intensity of the electric field $E(\mathbf{r})$ within $\mathcal{S}_\mathrm{R}$, $\int_{\mathcal{S}_\mathrm{R}} ||E(\mathbf{r})||^2\, d\mathbf{r}$, is maximized.

B. Maximum Coupling Intensity Between Intelligent Surfaces

The effect of each polarization direction can be studied separately if the components of $J(\mathbf{s}) = J_x(\mathbf{s})\,\hat{\mathbf{u}}_x + J_y(\mathbf{s})\,\hat{\mathbf{u}}_y + J_z(\mathbf{s})\,\hat{\mathbf{u}}_z$ are taken orthogonal. Therefore, without of generality, suppose we excite the x-component, i.e., $J(\mathbf{s}) = J_x(\mathbf{s})\,\hat{\mathbf{u}}_x$. By expanding $G(\mathbf{r}-\mathbf{s})$ in the basis sets $\{\phi_n(\mathbf{s})\}$ and $\{\psi_n(\mathbf{r})\}$, i.e., $G(\mathbf{r}-\mathbf{s}) = \sum_n \xi_n \phi_n(\mathbf{s}) \otimes \psi_n^\dagger(\mathbf{r})$, the total normalized (i.e., dimensionless) coupling intensity between intelligent surfaces results

$$\begin{aligned} c_x &= \frac{(4\pi)^2}{\lambda^2}\frac{1}{(\omega\mu)^2}\sum_n \xi_n^2 = \frac{4}{\eta^2}\int_{\mathcal{S}_\mathrm{R}}\int_{\mathcal{S}_\mathrm{T}} ||G_x(\mathbf{r}-\mathbf{s})||^2\, d\mathbf{r}\, d\mathbf{s} \\ &= \frac{1}{\lambda^2}\int_{\mathcal{S}_\mathrm{R}}\int_{\mathcal{S}_\mathrm{T}} \frac{(r_y-s_y)^2+(r_z-s_z)^2}{|\mathbf{r}-\mathbf{s}|^4}\, d\mathbf{r}\, d\mathbf{s}, \end{aligned} \tag{11}$$

where $\mathbf{r} = (r_x, r_y, r_z)$ and $\mathbf{s} = (s_x, s_y, s_z)$. The notation $G_x(\cdot)$ indicates we consider only the first column of tensor $G(\cdot)$, corresponding to the contribution caused by an excitation in the x-direction. Note that in general the excitation in the x-direction might contribute to all directions in the received electric field. The expressions for the other exciting directions are similars with mutual exchange of x, y and z.

In [18] the approximate solution to the eigenfunction problem valid for two collinear rectangular prisms at distance d, oriented along the z-axis, of volume $V_\mathrm{T} = \Delta x_\mathrm{T}\,\Delta y_\mathrm{T}\,\Delta z_\mathrm{T}$ and $V_\mathrm{R} = \Delta x_\mathrm{R}\,\Delta y_\mathrm{R}\,\Delta z_\mathrm{R}$, respectively, is presented. Specifically, the solution holds when the volumes are far apart compared to their sizes, i.e., $d \gg \Delta x_\mathrm{T}, \Delta y_\mathrm{T}, \Delta z_\mathrm{T}, \Delta x_\mathrm{R}, \Delta y_\mathrm{R}, \Delta z_\mathrm{R}$, which means they are in the (Fraunhofer) far-field region. In this case, the number of DoF available for communication have been found to be

$$D = \frac{\Delta x_\mathrm{T}\,\Delta y_\mathrm{T}\Delta x_\mathrm{R}\,\Delta y_\mathrm{R}}{d^2\lambda^2}, \tag{12}$$

whereas the total (un-normalized) coupling factor is

$$c \propto \frac{V_\mathrm{T}\,V_\mathrm{R}}{(4\pi d)^2}\,. \tag{13}$$

Note that the thickness of volumes in the z axis does not affect the number of DoF but only the coupling intensity.

Incidentally, for very small antennas, i.e., $\Delta x_\mathrm{T}\Delta x_\mathrm{R} \ll d\,\lambda$, $\Delta y_\mathrm{T}\Delta y_\mathrm{R} \ll d\,\lambda$, only one solution to the eigenfunctions problem exists, corresponding to a plane wave that travels with direction from the transmit antenna to the receive antenna. Unfortunately, the result above by [18] is no longer valid when analyzing a LIS as the assumption of far apart antennas, and hence the parallax approximation typical of the Fraunhofer region, does not hold anymore.

The analytical derivation of the eigenfunctions and eigenvalues in general is elusive and one has to resort to e.m. simulations, which could be prohibitive for LISs and typically they do not provide general insights. In the next sections we bypass the direct derivation of the solutions of the eigenfunction problem by resorting to geometric arguments, with the purpose to determine the number of DoF available for communication. Our aim is to derive simple expressions for LISs in particular geometric configurations of interest, also valid in the radiating near-field.

III. Communication DoF between Intelligent Surfaces

In this section, we derive approximate expressions for the communication DoF between a transmit SIS and a receive LIS antenna following 2D sampling theory arguments. The

accuracy of such expressions, with respect to the actual DoF value from the eigenfunction problem in Sec. II, is addressed in the numerical results.

Consider, without loss of generality, that the receive LIS $\mathcal{S}_\mathrm{R}$ is deployed along the xy-plane at $z = 0$. Therefore the generic point on the surface is represented by the coordinates $\mathbf{r} = (r_x, r_y, 0)$. Denote with $\mathbf{s} = (s_x, s_y, s_z)$ the coordinates of the generic point source of the transmit surface $\mathcal{S}_\mathrm{T}$. The wave originated by the point source $\mathbf{s}$ has wavenumber k_0 in the radial direction $\mathbf{r}-\mathbf{s}$ between the point source and the generic point $\mathbf{r}$ on the receive (observation) surface $\mathcal{S}_\mathrm{R}$. Contrarily to what happens in 1D coordinate systems, where a linear transformation never changes or generates new frequency components, when moving to 2D and 3D coordinate systems, it may happen that the observed wavenumber is different from k_0 if the observation direction is different from $\mathbf{r}-\mathbf{s}$. More specifically, along the x and y directions of the receive surface, the observed wave is characterized by wavenumber

$$\mathbf{k}(\mathbf{r},\mathbf{s}) = (k_x(\mathbf{r},\mathbf{s}), k_y(\mathbf{r},\mathbf{s}), 0) = \mathbf{r}-\mathbf{s}-\hat{\mathbf{n}}\left((\mathbf{r}-\mathbf{s})\cdot\hat{\mathbf{n}}\right), \quad (14)$$

where $\hat{\mathbf{n}}$ is the unit vector perpendicular to the surface in the point $\mathbf{r}$, so that

$$\begin{aligned} k_x(\mathbf{r},\mathbf{s}) &= k_0 \frac{r_x - s_x}{\sqrt{(r_x-s_x)^2+(r_y-s_y)^2+s_z^2}} \\ k_y(\mathbf{r},\mathbf{s}) &= k_0 \frac{r_y - s_y}{\sqrt{(r_x-s_x)^2+(r_y-s_y)^2+s_z^2}}. \end{aligned} \quad (15)$$

Consider now an infinitesimal surface $d\mathbf{r}$ centered in $\mathbf{r}$. The received wave observed in $\mathbf{r}$ can be seen as a two-dimensional signal whose local bandwidth changes slowly with $\mathbf{r}-\mathbf{s}$. The local bandwidth in the wavenumber domain observed in $\mathbf{r}$ is the maximum wavenumber spread related to all point sources in $\mathcal{S}_\mathrm{T}$. Specifically it is

$$B(\mathbf{r}) = \frac{1}{4}\mathrm{area}_{\mathbf{s}\in\mathcal{S}_\mathrm{T}}\left[\mathbf{k}(\mathbf{r},\mathbf{s})\right], \quad (16)$$

where the operator $\mathrm{area}_{\mathbf{s}\in\mathcal{S}_\mathrm{T}}[\cdot]$ returns the area of the region in the complex plane spanned by the function $\mathbf{k}(\mathbf{r},\mathbf{s})$ when parameter $\mathbf{s}$ varies in $\mathcal{S}_\mathrm{T}$.

Considering that the DoF (i.e., the number of requested samples at Nyquist rate) of a 2D signal of (spatial) bandwidth B in an area S is, as first order approximation, equal to $\frac{BS}{\pi^2}$, the number of dimensions of the signal "projected" onto $\mathcal{S}_\mathrm{R}$ results

$$D = \frac{1}{\pi^2}\int_{\mathcal{S}_\mathrm{R}} B(\mathbf{r})\, d\mathbf{r}. \quad (17)$$

In the next section we make (17) particular to some LIS configurations with the purpose to derive simple expressions of the DoF and obtain some interesting insights. Such expressions can be of interest when planning a wireless network based on intelligent surfaces.

IV. Case Study

Due to the lack of space, in this section we make (11) and (17) particular to the significant case of parallel intelligent surfaces with the purpose to derive simple expressions of the gain and DoF and obtain some interesting insights.

Consider a transmit MIS/SIS and a receive LIS at distance d. This situation is expected to be common in practice where the MIS/SIS antenna might be embedded, for instance, into a smartphone or on top of a car, whereas the LIS coats a wall of a building. The centers and sizes of the transmit and receive intelligent surfaces are, respectively, $\mathbf{s}_0 = (x_0, y_0, d)$, $(L_\mathrm{x}, L_\mathrm{y})$ and $(0,0,0)$, $(S_\mathrm{x}, S_\mathrm{y})$. The corresponding areas are $A_\mathrm{T} = L_\mathrm{x}\, L_\mathrm{y}$ and $A_\mathrm{R} = S_\mathrm{x}\, S_\mathrm{y}$. Since the transmit antenna is a MIS/SIS, it is reasonable to assume that $L_\mathrm{x}, L_\mathrm{y} \ll d$, $L_\mathrm{x} \ll S_\mathrm{x}$, and $L_\mathrm{y} \ll S_\mathrm{y}$. Contrarily, S_x and S_y may be of the same order of magnitude as d.

A. Power Gain Between Communicating LIS and SIS

The coupling intensity for any generic geometric configuration of antennas can be easily obtained by solving (11) numerically. Nevertheless, closed-form expressions can be obtained for some relevant cases from which some interesting insights can be derived.

To calculate the power gain between the transmit SIS and the receive LIS, one has to consider only the component in (11) perpendicular to the surface, i.e.,

$$\begin{aligned} g &= \frac{1}{\lambda^2}\int_{\mathcal{S}_\mathrm{R}}\int_{\mathcal{S}_\mathrm{T}} \frac{(r_y-s_y)^2+(r_z-s_z)^2}{|\mathbf{r}-\mathbf{s}|^4}\hat{\mathbf{p}}\cdot\hat{\mathbf{n}}\, d\mathbf{r}\, d\mathbf{s} \\ &\simeq \frac{A_\mathrm{T}}{\lambda^2}\int_{\mathcal{S}_\mathrm{R}} \frac{\left((r_y-y_0)^2+d^2\right)\, d}{|\mathbf{r}-\mathbf{s}_0|^5}\, d\mathbf{r}, \end{aligned} \quad (18)$$

where $\hat{\mathbf{p}} = (\mathbf{r}-\mathbf{s})/|\mathbf{r}-\mathbf{s}|$, and $\hat{\mathbf{n}} = \hat{\mathbf{z}}$. In (18), we have made the approximations $s_z \simeq d$ and $|\mathbf{r}-\mathbf{s}|^2 \simeq |\mathbf{r}-\mathbf{s}_0|^2$, since the transmit antenna is small compared to the distance d. As a consequence, the result does not depend on SIS orientation but only on its area A_T. Equation (18) can be solved in closed-form but the final expression is quite long and it does not provide important insights. Therefore, for the sake of space, we report here the result valid for $\mathbf{s}_0 = (0,0,d)$ from which some interesting conclusions can be drawn. In this case, (18) becomes

$$\begin{aligned} g &= \frac{A_\mathrm{T}}{\lambda^2}\int_{-S_\mathrm{x}/2}^{S_\mathrm{x}/2}\int_{-S_\mathrm{y}/2}^{S_\mathrm{y}/2} \frac{d\left(r_y^2+d^2\right)}{\left(r_x^2+r_y^2+d^2\right)^{5/2}}\, dr_x\, dr_y \\ &= \frac{4d\, A_\mathrm{T} S_\mathrm{x}}{3\lambda^2}\int_{-S_\mathrm{y}/2}^{S_\mathrm{y}/2} \frac{6d^2+S_\mathrm{x}^2+6r_y^2}{\left(d^2+r_y^2\right)\left(4d^2+S_\mathrm{x}^2+4r_y^2\right)^{3/2}}\, dr_y, \end{aligned} \quad (19)$$

which gives

$$\begin{aligned} g &= \frac{8A_\mathrm{T}}{3\lambda^2} \\ &\cdot\left(\frac{S_\mathrm{x}S_\mathrm{y}\, d}{\left(S_\mathrm{x}^2+4d^2\right)\sqrt{S_\mathrm{x}^2+S_\mathrm{y}^2+4d^2}} + \tan^{-1}\left(\frac{S_\mathrm{x}S_\mathrm{y}}{2d\sqrt{S_\mathrm{x}^2+S_\mathrm{y}^2+4d^2}}\right)\right). \end{aligned} \quad (20)$$

For a squared LIS, the last expression simplifies as follows

$$g = \frac{4A_{\mathrm{T}}}{3\lambda^2}\left(\frac{\sqrt{2F}}{\sqrt{1+2F}(1+4F)} + 2\mathrm{acot}\left(\sqrt{8F(1+2F)}\right)\right), \quad (21)$$

where $F = \frac{d^2}{A_{\mathrm{R}}}$. It can be observed from (21) that the gain is a function of relative geometric quantities, i.e., the normalized (to the wavelength) transmit SIS' area A_{T} and the ratio F.

It is interesting to analyze the behavior of (21) when the LIS is extremely large compared to the distance d (small F), that is

$$g^{(\text{large LIS})} = \frac{4\pi A_{\mathrm{T}}}{3\lambda^2}, \quad (22)$$

which becomes independent of the distance. Instead, for large distances (large F), corresponding to the Fraunhofer far-field region, (21) gives

$$g^{(\text{large } d)} = \frac{A_{\mathrm{T}} A_{\mathrm{R}}}{\lambda^2 d^2}. \quad (23)$$

The latter is the result found by Miller [18] (reported in (13) with a different normalization factor) when considering thin volumes and it is nothing else than the well-known Friis' formula [16]. In fact, if one defines $G_{\mathrm{I}} = \lambda^2/(4\pi d)^2$, $G_{\mathrm{T}} = 4\pi A_{\mathrm{T}}/\lambda^2$, and $G_{\mathrm{R}} = 4\pi A_{\mathrm{R}}/\lambda^2$, respectively, the isotropic free-space channel gain, the gain of the transmit and receive antennas considered as aperture antennas, it is $g^{(\text{large } d)} = G_{\mathrm{T}}\, G_{\mathrm{R}}\, G_{\mathrm{I}}$.

Equation (18) and, in particular, (20) and (21) represent simple design formulas useful to characterize the link budget in LIS-based communications without resorting to e.m. extensive simulations.

B. DoF of Communicating Parallel LIS/SIS

For parallel intelligent surfaces, a way to compute (16) is to approximate the curve delimiting $\mathrm{area}_{\mathbf{s}\in\mathcal{S}_{\mathrm{T}}}[\mathbf{k}(\mathbf{r},\mathbf{s})]$ with a quadrilateral having vertices given by $k_x^{(i)}(\mathbf{r}) = k_x\left(\mathbf{r},\mathbf{s}^{(i)}\right)$, $k_y^{(i)}(\mathbf{r}) = k_y\left(\mathbf{r},\mathbf{s}^{(i)}\right)$, $i = 1,2,\ldots,5$, with $\mathbf{s}^{(1)} = (x_0 - L_{\mathrm{x}}/2, y_0 - L_{\mathrm{y}}/2, d)$, $\mathbf{s}^{(2)} = (x_0 + L_{\mathrm{x}}/2, y_0 - L_{\mathrm{y}}/2, d)$, $\mathbf{s}^{(3)} = (x_0 - L_{\mathrm{x}}/2, y_0 + L_{\mathrm{y}}/2, d)$, $\mathbf{s}^{(4)} = (x_0 + L_{\mathrm{x}}/2, y_0 + L_{\mathrm{y}}/2, d)$, $\mathbf{s}^{(5)} = \mathbf{s}^{(1)}$, and then by applying the Gauss' formula

$$A(\mathbf{r}) \simeq \frac{1}{2}\left|\sum_{i=1}^{4}\left(k_x^{(i)}(\mathbf{r})\, k_y^{(i+1)}(\mathbf{r}) - k_x^{(i+1)}(\mathbf{r})\, k_y^{(i)}(\mathbf{r})\right)\right|. \quad (24)$$

From (16) and (17) it follows that

$$D^{||} \simeq \frac{1}{4\pi^2}\int_{\mathcal{S}_{\mathrm{R}}} A(\mathbf{r})\, d\mathbf{r}. \quad (25)$$

Unfortunately, (25) does not admit a closed-form expression in general. However, even though it requires the evaluation of a two-folded integral, its numerical computation is very fast and it does not pose any particular issue compared to the numerical complexity of the eigenfunction problem (5) and (6).

Nevertheless, it could be of interest to derive closed-form expressions of (25) for some significant cases. Specifically, since $L_{\mathrm{x}}, L_{\mathrm{y}} \ll d$, setting $x_0 = y_0 = 0$, the integrand (24) can be approximated with the first-order Taylor double series expansion in L_{x} and L_{y} resulting in

$$D^{||} \simeq \frac{2L_{\mathrm{x}}L_{\mathrm{y}}}{\lambda^2}\left(\frac{S_{\mathrm{x}}\tan^{-1}\left(\frac{S_{\mathrm{y}}}{\sqrt{4d^2+S_{\mathrm{x}}^2}}\right)}{\sqrt{4d^2+S_{\mathrm{x}}^2}} + \frac{S_{\mathrm{y}}\tan^{-1}\left(\frac{S_{\mathrm{x}}}{\sqrt{4d^2+S_{\mathrm{y}}^2}}\right)}{\sqrt{4d^2+S_{\mathrm{y}}^2}}\right). \quad (26)$$

For $d \gg S_{\mathrm{x}}, S_{\mathrm{y}}$, i.e., in the far-field region, it is

$$D^{||}_{\text{large}} = \frac{A_{\mathrm{T}}A_{\mathrm{R}}}{\lambda^2 d^2}, \quad (27)$$

which gives (12) derived in [18].

The limit of (26) for $S_{\mathrm{x}}, S_{\mathrm{y}} \to \infty$, i.e., very large surfaces, is

$$D^{||}_{\text{asympt}} = \frac{\pi\, L_{\mathrm{x}}\, L_{\mathrm{y}}}{\lambda^2} = \frac{\pi A_{\mathrm{T}}}{\lambda^2}. \quad (28)$$

Equation (28) indicates that the maximum number of DoF depends only on the area of the transmit surface (normalized to the square half-wavelength), i.e., the area of the smallest of the 2 antennas, and it represents the ultimate DoF limit which is independent of the distance. This result is reminiscent of the DoF in MIMO systems when the channel matrix is full rank, i.e., in the presence of rich multipath [3]. Unfortunately, in line-of-sight (LOS) channel condition, the rank of the channel matrix is 1, and hence $D = 1$ (only beamforming gain is present). Instead, result (26) indicates that with a LIS one can obtain a number of DoF larger than 1 even in LOS. Having large DoF in LOS could significantly increase the link capacity, especially at millimeter waves or in the THz band where the multipath is not rich or could be dominated by the LOS component.

A more extensive analysis for other geometric configurations can be found in the extended journal version of the paper [20].

V. Numerical results

In this section, we propose some numerical examples with the purpose to illustrate the potential advantages in communicating with LISs and to assess the validity of the proposed method.

In Fig. 2, the total link gain between a SIS communicating with a LIS using (20), normalized to $G_{\mathrm{T}} = 4\pi A_{\mathrm{T}}/\lambda^2$, is shown as a function of F and for different values of LIS' aspect ratio $\mathrm{AR} = S_{\mathrm{x}} : S_{\mathrm{y}}$. Notice that this plot does not depend on λ and on the absolute distance between the intelligent surfaces and the dimension of the receive LIS, but only on the relative quantities $F = d^2/A_{\mathrm{R}}$ and AR. When the size of the LIS is comparable or larger than the distance from the transmitter (small F), near-field effects become dominant leading to a saturation of the link gain toward the limit value (22). This can be ascribed to diffraction effects, which make the commonly used antenna aperture formula, according to which the antenna gain is proportional to the geometric area, no longer valid. From Fig. 2, it can be also noticed that the best geometric

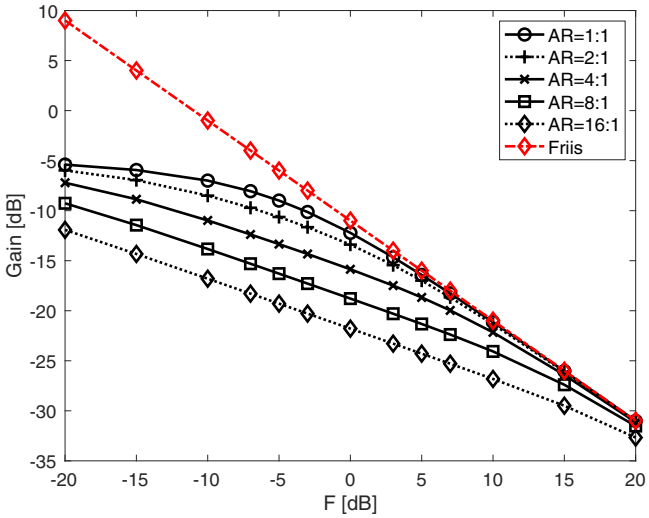

Fig. 2. Normalized gain vs $F = d^2/A_R$ of a SIS-LIS link.

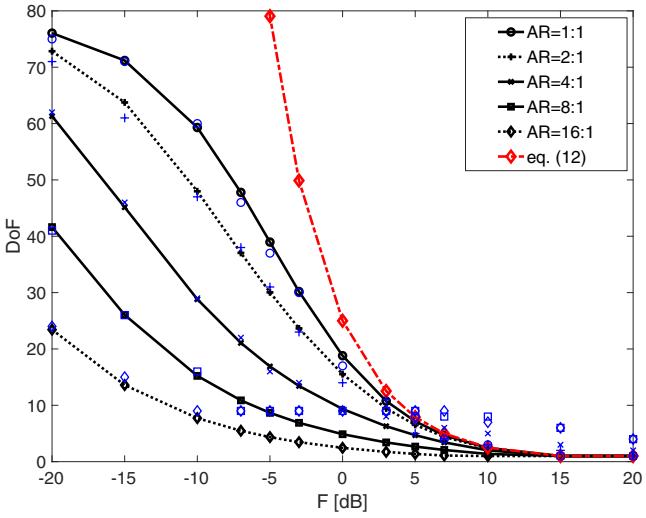

Fig. 3. DoF vs $F = d^2/A_R$ for parallel surfaces. $A_R = 25\,\text{cm}^2$, $f_c = 28\,\text{GHz}$.

shape is the square one (AR = 1 : 1). For comparison, the gain obtained using the Friis' formula (23) (normalized to G_T) is also shown, from which it is evident that it fails in modeling the link budget when LISs are used, especially for low F.

Now we investigate the number of DoF available when a LIS and a SIS are communicating in the near- and far-field. Fig. 3 shows the DoF in (26) related to parallel surfaces as a function of F for different values of AR, with $\lambda = 1\,\text{cm}$ (28 GHz), and $5 \times 5\,\text{cm}^2$ LIS ($A_R = 25\,\text{cm}^2$).[3]

For low F (very large LIS), the number of DoF saturates to the limit value given by (28), in this case equal to 100. As far as the Fraunhofer far-field regime is approached (large F), the number of DoF tends to one, as in conventional MIMO systems in LOS condition where only the beamforming gain is present. Again, the best LIS configuration is given by the square shape (AR = 1 : 1). The result obtained using (12) by [18] is also reported. It is evident how this expression, valid for antennas at distances much larger than their dimension, is not accurate for small F and it is not able to capture the effect of the aspect ratio of the LIS.

In order to validate the approach proposed in Sec. III, results have been compared to those obtained by solving numerically the eigenfunction problem in Sec. II. To this purpose, different numerical approximation methods exist (e.g., Galerkin's method) [19]. Among them, we considered the following one: we decomposed each surface in very small square patches of side $\Delta = \lambda/16$ and we considered them as piece-wise constant basis functions for the surfaces. In this way, the eigenfunction problem can be approximated into a singular value decomposition problem with dimension $A_R/\Delta^2 \times A_T/\Delta^2$. Unfortunately, such a method becomes intractable as soon as the surfaces become large compared to λ due to the corresponding huge dimension of the matrix to decompose. To make the computation affordable (a few days computation time), we considered a relative small LIS with $A_R = 1\,\text{m}^2$. The number of DoF has been computed by considering the largest eigenvalues within a tolerance of 3dB. Results are plotted in Fig. 3 (blue markers) and show a good agreement with the model developed in Sec. III, especially for small F. For large F, there are some discrepancies, but the fact that our results are consistent with the analytical expression (12), which is accurate for large F, generates the suspect of numerical evaluation issues caused by the singular-value decomposition of huge likely ill-posed matrices.

Interestingly, from the above results it turns out that DoF significantly larger than 1 can be obtained at practical distances in LOS channel condition, which can have important implications in next generation wireless networks operating at millimeter wave and THz bands. For instance, suppose a typical industrial scenario is considered, where a LIS of size $5 \times 5\,\text{m}^2$ is deployed on the factory ceiling at heigh $d = 5\,\text{m}$. From Fig. 3, it follows that the achievable DoF, supposing transmitting sensors equipped with SIS of area $A_T = 25\,\text{cm}^2$ located close to the floor, is $D \simeq 20$ ($F = 0\,\text{dB}$, AR = 1 : 1). This might correspond to a significant increase of link capacity with respect to the situation where only beamforming gain is exploited and $D = 1$.

This result can be interpreted also from another point of view: in fact, equivalently up to $D/A_T \simeq 8,000$ orthogonal links per square meter can be activated, which is very promising for the factories of the future where extremely high nodes density values are expected. In addition, the possibility of making wireless links orthogonal at e.m. level, simplifies the channel multiple access, thus significantly reducing the communication latency.

[3]Although the values obtained from (26) should be rounded to the nearest integer value larger or equal to 1, here the continuous version is plotted to easy the reading.

VI. Conclusion

We have shown that the optimal communication between LIS/SIS can be formulated as an eigenfunction problem starting from e.m. arguments. To obtain high-level descriptions of LIS-based communication and to avoid extensive and sometimes prohibitive e.m.-level simulations, simple but accurate analytical expressions for the link gain and the available orthogonal communication modes (i.e., DoF) between the transmitter and the receiver are derived. The obtained expressions allow to get important insights about the communication between intelligent surfaces and can serve as design guidelines in future wireless networks employing LISs.

In particular, it has been shown that the achievable DoF and gain offered by the LIS-enabled wireless link are determined only by geometric factors normalized to the wavelength, and that the classic Friis' formula is no longer valid in this scenario. The fundamental limits for very large intelligent surfaces have been found to be dependent only on the normalized area of the smallest antenna involved in the communication.

One important result is that using LISs one can can exploit the spatial multiplexing even in LOS channel condition at practical distances, contrarily to conventional MIMO systems that can only exploit signal-to-noise ratio (SNR) enhancement (beamforming) when in strong LOS. This opens the possibility to satisfy the challenging requirements of next generation wireless networks in terms of massive communications and high capacity per square meter.

Acknowledgment

This paper has received funding from the ATTRACT project funded by the EC under Grant Agreement 777222.

References

[1] S. Vitturi, C. Zunino, and T. Sauter, "Industrial communication systems and their future challenges: Next-generation ethernet, IIoT, and 5G," *Proceedings of the IEEE*, vol. 107, no. 6, pp. 944–961, June 2019.

[2] E. Björnson, L. Sanguinetti, H. Wymeersch, J. Hoydis, and T. L. Marzetta, "Massive MIMO is a reality - what is next?: Five promising research directions for antenna arrays," *Digital Signal Processing*, 2019. [Online]. Available: http://www.sciencedirect.com/science/article/pii/S1051200419300776

[3] D. Tse and P. Viswanath, *Fundamentals of Wireless Communications*. New York, NY: Cambridge University Press, 2005.

[4] A. Silva, F. Monticone, G. Castaldi, V. Galdi, A. Alù, and N. Engheta, "Performing mathematical operations with metamaterials," *Science*, vol. 343, no. 6167, pp. 160–163, 2014. [Online]. Available: https://science.sciencemag.org/content/343/6167/160

[5] S. A. Tretyakov, "Metasurfaces for general transformations of electromagnetic fields," *Philosophical Transactions of the Royal Society A: Mathematical, Physical and Engineering Sciences*, vol. 373, Aug 2015. [Online]. Available: https://doi.org/10.1098/rsta.2014.0362

[6] L. Di Palma, A. Clemente, L. Dussopt, R. Sauleau, P. Potier, and P. Pouliguen, "Circularly-polarized reconfigurable transmitarray in Ka-band with beam scanning and polarization switching capabilities," *IEEE Transactions on Antennas and Propagation*, vol. 65, no. 2, pp. 529–540, Feb 2017.

[7] P. Nepa and A. Buffi, "Near-field-focused microwave antennas: Near-field shaping and implementation." *IEEE Antennas and Propagation Magazine*, vol. 59, no. 3, pp. 42–53, June 2017.

[8] N. Shlezinger, O. Dicker, Y. C. Eldar, I. Yoo, M. F. Imani, and D. R. Smith, "Dynamic Metasurface Antennas for Uplink Massive MIMO Systems," *arXiv e-prints*, p. arXiv:1901.01458, Jan 2019.

[9] C. Liaskos, S. Nie, A. Tsioliaridou, A. Pitsillides, S. Ioannidis, and I. Akyildiz, "A new wireless communication paradigm through software-controlled metasurfaces," *IEEE Communications Magazine*, vol. 56, no. 9, pp. 162–169, Sep. 2018.

[10] M. D. Renzo, M. Debbah, D.-T. Phan-Huy, A. Zappone, M.-S. Alouini, C. Yuen, V. Sciancalepore, G. C. Alexandropoulos, J. Hoydis, H. Gacanin, J. d. Rosny, A. Bounceur, G. Lerosey, and M. Fink, "Smart radio environments empowered by reconfigurable AI meta-surfaces: an idea whose time has come," *EURASIP Journal on Wireless Communications and Networking*, vol. 2019, no. 1, p. 129, 2019. [Online]. Available: https://doi.org/10.1186/s13638-019-1438-9

[11] S. V. Hum and J. Perruisseau-Carrier, "Reconfigurable reflectarrays and array lenses for dynamic antenna beam control: A review," *IEEE Transactions on Antennas and Propagation*, vol. 62, no. 1, pp. 183–198, Jan 2014.

[12] L. Zhang, X. Q. Chen, S. Liu, Q. Zhang, J. Zhao, J. Y. Dai, G. D. Bai, X. Wan, Q. Cheng, G. Castaldi, V. Galdi, and T. J. Cui, "Space-time-coding digital metasurfaces," *Nature Communications*, vol. 9, no. 1, p. 4334, 2018. [Online]. Available: https://doi.org/10.1038/s41467-018-06802-0

[13] S. Hu, F. Rusek, and O. Edfors, "Beyond massive MIMO: The potential of data transmission with large intelligent surfaces," *IEEE Transactions on Signal Processing*, vol. 66, no. 10, pp. 2746–2758, May 2018.

[14] R. F. Harrington, *Time-Harmonic Electromagnetic Fields*. New York, USA: IEEE Press - Wiley, 2001.

[15] M. Franceschetti, *Wave Theory of Information*. Cambridge, UK: Cambridge University press, 2018.

[16] C. A. Balanis, *Antenna Theory: analysis and design*. New Jersey, USA: Wiley, 2016.

[17] A. S. Y. Poon, R. W. Brodersen, and D. N. C. Tse, "Degrees of freedom in multiple-antenna channels: a signal space approach," *IEEE Transactions on Information Theory*, vol. 51, no. 2, pp. 523–536, Feb 2005.

[18] D. A. B. Miller, "Communicating with waves between volumes: evaluating orthogonal spatial channels and limits on coupling strengths," *Appl. Opt.*, vol. 39, no. 11, pp. 1681–1699, Apr 2000. [Online]. Available: http://ao.osa.org/abstract.cfm?URI=ao-39-11-1681

[19] R. Piestun and D. A. B. Miller, "Electromagnetic degrees of freedom of an optical system," *J. Opt. Soc. Am. A*, vol. 17, no. 5, pp. 892–902, May 2000. [Online]. Available: http://josaa.osa.org/abstract.cfm?URI=josaa-17-5-892

[20] D. Dardari, "Communicating with large intelligent surfaces: Fundamental limits and models," *ArXiv*, vol. abs/1912.01719, 2019, submitted.